Femtosecond high-power quantum dot vertical external cavity surface emitting laser

Martin Hoffmann,[1,*] Oliver D. Sieber,[1] Valentin J. Wittwer,[1] Igor L. Krestnikov,[2] Daniil A. Livshits,[2] Yohan Barbarin,[1] Thomas Südmeyer,[1] and Ursula Keller[1]

[1]*Department of Physics, ETH Zurich, Wolfgang-Pauli-Strasse 16, 8093 Zurich, Switzerland*
[2]*Innolume GmbH, Konrad-Adenauer-Allee 11, 44263 Dortmund, Germany*
**mh@phys.ethz.ch*

Abstract: We report on the first femtosecond vertical external cavity surface emitting laser (VECSEL) exceeding 1 W of average output power. The VECSEL is optically pumped, based on self-assembled InAs quantum dot (QD) gain layers, cooled efficiently using a thin disk geometry and passively modelocked with a fast quantum dot semiconductor saturable absorber mirror (SESAM). We developed a novel gain structure with a flat group delay dispersion (GDD) of ± 10 fs^2 over a range of 30 nm around the designed operation wavelength of 960 nm. This amount of GDD is several orders of magnitude lower compared to standard designs. Furthermore, we used an optimized positioning scheme of 63 QD gain layers to broaden and flatten the spectral gain. For stable and self-starting pulse formation, we have employed a QD-SESAM with a fast absorption recovery time of around 500 fs. We have achieved 1 W of average output power with 784-fs pulse duration at a repetition rate of 5.4 GHz. The QD-SESAM and the QD-VECSEL are operated with similar cavity mode areas, which is beneficial for higher repetition rates and the integration of both elements into a modelocked integrated external-cavity surface emitting laser (MIXSEL).

OCIS codes: (140.7260) Vertical cavity surface emitting lasers; (140.4050) Mode-locked lasers.

References and links

1. U. Keller, and T. H. Chiu, "Resonant passive modelocked Nd:YLF laser," IEEE J. Quantum Electron. **28**(7), 1710–1721 (1992).
2. U. Keller, K. J. Weingarten, F. X. Kärtner, D. Kopf, B. Braun, I. D. Jung, R. Fluck, C. Hönninger, N. Matuschek, and J. Aus der Au, "Semiconductor saturable absorber mirrors (SESAMs) for femtosecond to nanosecond pulse generation in solid-state lasers," IEEE J. Sel. Top. Quantum Electron. **2**(3), 435–453 (1996).
3. U. Keller, "Ultrafast solid-state laser oscillators: a success story for the last 20 years with no end in sight," Appl. Phys. B **100**(1), 15–28 (2010).
4. U. Keller, and A. C. Tropper, "Passively modelocked surface-emitting semiconductor lasers," Phys. Rep. **429**(2), 67–120 (2006).
5. D. J. H. C. Maas, A.-R. Bellancourt, B. Rudin, M. Golling, H. J. Unold, T. Südmeyer, and U. Keller, "Vertical integration of ultrafast semiconductor lasers," Appl. Phys. B **88**(4), 493–497 (2007).
6. A.-R. Bellancourt, D. J. H. C. Maas, B. Rudin, M. Golling, T. Südmeyer, and U. Keller, "Modelocked Integrated External-Cavity Surface Emitting Laser," IET Optoelectron. **3**(2), 61–72 (2009).
7. A. Giesen, H. Hügel, A. Voss, K. Wittig, U. Brauch, and H. Opower, "Scalable Concept for Diode-Pumped High-Power Solid-State Lasers," Appl. Phys. B **58**, 365–372 (1994).
8. D. Lorenser, D. J. H. C. Maas, H. J. Unold, A.-R. Bellancourt, B. Rudin, E. Gini, D. Ebling, and U. Keller, "50-GHz passively mode-locked surface-emitting semiconductor laser with 100 mW average output power," IEEE J. Quantum Electron. **42**(8), 838–847 (2006).
9. P. Klopp, U. Griebner, M. Zorn, A. Klehr, A. Liero, M. Weyers, and G. Erbert, "Mode-locked InGaAs-AlGaAs disk laser generating sub-200-fs pulses, pulse picking and amplification by a tapered diode amplifier," Opt. Express **17**(13), 10820–10834 (2009).
10. A. Aschwanden, D. Lorenser, H. J. Unold, R. Paschotta, E. Gini, and U. Keller, "2.1-W picosecond passively mode-locked external-cavity semiconductor laser," Opt. Lett. **30**(3), 272–274 (2005).

#140557 - $15.00 USD Received 4 Jan 2011; accepted 29 Mar 2011; published 13 Apr 2011

11. B. Rudin, V. J. Wittwer, D. J. H. C. Maas, M. Hoffmann, O. D. Sieber, Y. Barbarin, M. Golling, T. Südmeyer, and U. Keller, "High-power MIXSEL: an integrated ultrafast semiconductor laser with 6.4 W average power," Opt. Express **18**(26), 27582–27588 (2010).
12. K. G. Wilcox, Z. Mihoubi, G. J. Daniell, S. Elsmere, A. Quarterman, I. Farrer, D. A. Ritchie, and A. Tropper, "Ultrafast optical Stark mode-locked semiconductor laser," Opt. Lett. **33**(23), 2797–2799 (2008).
13. D. J. H. C. Maas, A. R. Bellancourt, M. Hoffmann, B. Rudin, Y. Barbarin, M. Golling, T. Südmeyer, and U. Keller, "Growth parameter optimization for fast quantum dot SESAMs," Opt. Express **16**(23), 18646–18656 (2008).
14. A.-R. Bellancourt, Y. Barbarin, D. J. H. C. Maas, M. Shafiei, M. Hoffmann, M. Golling, T. Südmeyer, and U. Keller, "Low saturation fluence antiresonant quantum dot SESAMs for MIXSEL integration," Opt. Express **17**(12), 9704–9711 (2009).
15. K. G. Wilcox, M. Butkus, I. Farrer, D. A. Ritchie, A. Tropper, and E. U. Rafailov, "Subpicosecond quantum dot saturable absorber mode-locked semiconductor disk laser," Appl. Phys. Lett. **94**(25), 3 (2009).
16. L. Harris, D. J. Mowbray, M. S. Skolnick, M. Hopkinson, and G. Hill, "Emission spectra and mode structure of InAs/GaAs self-organized quantum dot lasers," Appl. Phys. Lett. **73**(7), 969–971 (1998).
17. B. Braun, K. J. Weingarten, F. X. Kärtner, and U. Keller, "Continuous-wave mode-locked solid-state lasers with enhanced spatial hole-burning, Part I: Experiments," Appl. Phys. B **61**, 429–437 (1995).
18. F. X. Kärtner, B. Braun, and U. Keller, "Continuous-wave-mode-locked solid-state lasers with enhanced spatial hole-burning, Part II: Theory," Appl. Phys. B **61**(6), 569–579 (1995).
19. M. Hoffmann, Y. Barbarin, D. J. H. C. Maas, M. Golling, I. L. Krestnikov, S. S. Mikhrin, A. R. Kovsh, T. Südmeyer, and U. Keller, "Modelocked quantum dot vertical external cavity surface emitting laser," Appl. Phys. B **93**(4), 733–736 (2008).
20. A. Aschwanden, D. Lorenser, H. J. Unold, R. Paschotta, E. Gini, and U. Keller, "10-GHz passively mode-locked surface emitting semiconductor laser with 1.4-W average output power," Appl. Phys. Lett. **86**(13), 131102 (2005).
21. P. Klopp, F. Saas, M. Zorn, M. Weyers, and U. Griebner, "290-fs pulses from a semiconductor disk laser," Opt. Express **16**(8), 5770–5775 (2008).
22. A. Garnache, S. Hoogland, A. C. Tropper, I. Sagnes, G. Saint-Girons, and J. S. Roberts, "Sub-500-fs soliton pulse in a passively mode-locked broadband surface-emitting laser with 100-mW average power," Appl. Phys. Lett. **80**(21), 3892–3894 (2002).
23. K. G. Wilcox, A. H. Quarterman, H. Beere, D. A. Ritchie, and A. C. Tropper, "High Peak Power Femtosecond Pulse Passively Mode-Locked Vertical-External-Cavity Surface-Emitting Laser," IEEE Photon. Technol. Lett. **22**(14), 1021–1023 (2010).
24. M. Lumb, P. Stavrinou, E. Clarke, R. Murray, C. Leburn, C. Jappy, N. Metzger, C. Brown, and W. Sibbett, "Dispersionless saturable absorber mirrors with large modulation depths and low saturation fluences," Appl. Phys. B **97**(1), 53–60 (2009).
25. M. Hoffmann, O. D. Sieber, D. J. H. C. Maas, V. J. Wittwer, M. Golling, T. Südmeyer, and U. Keller, "Experimental verification of soliton-like pulse-shaping mechanisms in passively mode-locked VECSELs," Opt. Express **18**(10), 10143–10153 (2010).
26. D. J. H. C. Maas, B. Rudin, A.-R. Bellancourt, D. Iwaniuk, S. V. Marchese, T. Südmeyer, and U. Keller, "High precision optical characterization of semiconductor saturable absorber mirrors," Opt. Express **16**(10), 7571–7579 (2008).
27. P. Langlois, M. Joschko, E. R. Thoen, E. M. Koontz, F. X. Kärtner, E. P. Ippen, and L. A. Kolodziejski, "High fluence ultrafast dynamics of semiconductor saturable absorber mirrors," Appl. Phys. Lett. **75**(24), 3841–3843 (1999).
28. R. Häring, R. Paschotta, A. Aschwanden, E. Gini, F. Morier-Genoud, and U. Keller, "High–power passively mode–locked semiconductor lasers," IEEE J. Quantum Electron. **38**(9), 1268–1275 (2002).

1. Introduction

We have made significant progress in compact ultrafast lasers with the invention and development of semiconductor saturable absorbers mirrors (SESAMs [1–3]), a family of optical devices that allow for very simple, self-starting passive modelocking of ultrafast diode-pumped solid-state lasers. The extension of this work towards ultrafast optically pumped vertical external cavity surface emitting laser (VECSEL) [4] provides further improvements in fabrication costs [5, 6]. We expect that these novel ultrafast semiconductor lasers will enable many commercial applications in the gigahertz pulse repetition rate regime. Here we have demonstrated for the first time high-power optically pumped femtosecond VECSELs with more than 1 W of average output power. Moreover, pulses as short as 416-fs could be achieved with more than 100 mW of average power which are particularly interesting for applications such as multi-photon microscopy, micro-machining and the generation of stable frequency combs for metrology applications.

#140557 - $15.00 USD Received 4 Jan 2011; accepted 29 Mar 2011; published 13 Apr 2011

Ultrafast VECSELs are a promising alternative to diode pumped solid-state lasers as they offer the possibility for cost-efficient mass production using a simple and compact laser cavity setup with both the semiconductor gain and absorber integrated within one wafer (i.e. the modelocked integrated external cavity surface emitting laser – MIXSEL) [5, 6]. Furthermore, they benefit from the power scalability of the thin disk geometry [7] and general semiconductor properties such as large wavelength flexibility with bandgap engineering and epitaxial growth techniques. Modelocked VECSELs have achieved impressive performance: a pulse repetition rate of 50 GHz [8], a pulse duration of 190 fs [9] and an average output power of 2.1 W [10] with a hybrid SESAM-VECSEL combination, and 6.4 W with a MIXSEL [11].

To date the generation of sub-picosecond pulses mostly relied on SESAMs with quantum well (QW) absorbers, whereas SESAMs with quantum dot (QD) saturable absorbers were mainly used for modelocking at high repetition rates [8] or in MIXSELs [11]. QW-SESAMs using the optical Stark effect and/or surface recombination can exhibit fast recovery dynamics, which allow for the generation of pulse durations well below 500 fs [9, 12]. QD-SESAMs, on the other hand, have the advantage of a low saturation fluence [13] which enabled modelocking in an anti-resonant MIXSEL [14]. In 2009, the first sub-picosecond QW-VECSEL modelocked using a QD-SESAM was realized, achieving 870 fs pulses and 45 mW of output power [15]. The recovery time of the QD-SESAM was around 800 fs, demonstrating that QD-SESAMs can also provide fast recovery dynamics. However, further studies on the effects of growth parameters was required [13]. To date most VECSELs have been based on QW gain layers. However, QD gain layers based on self-assembled InAs QDs inherently exhibit strong inhomogeneous gain broadening [16], which increases the gain bandwidth and therefore should support shorter pulse durations [17, 18]. The first modelocked QD-VECSEL was demonstrated in 2008 generating a pulse duration of 18 ps with an average output power of 27 mW [19]. In this proof-of-principle result, a QW-SESAM was used for modelocking.

In Tab. 1 and Fig. 1 the performance of different VECSELs based on QW and QD gain layers are compared. So far, all femtosecond VECSELs have operated in a limited average output power regime below 200 mW which is not sufficient for many applications. In this paper we demonstrate the first femtosecond operation of a modelocked VECSEL at 1 W average output power. Both the SESAM and the gain element are based on QDs. The structure was designed for both large gain bandwidth and low dispersion to support shorter pulses. The implemented optimizations will be discussed in detail in the following sections. We achieved 1.05 W of average output power with a pulse duration of 784 fs at a center wavelength of 970 nm. Shorter pulses could also be obtained with pulse durations as short as 416 fs at 143 mW of output power. These are the shortest pulses which have been reported from either an ultrafast QD-VECSEL or a QD-SESAM modelocked VECSEL.

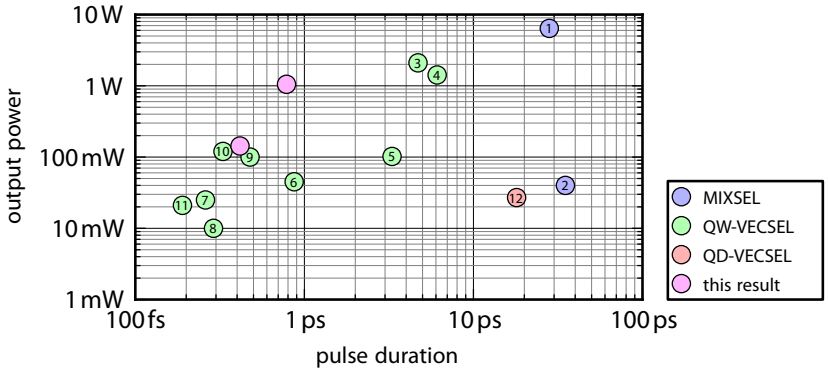

Fig. 1. Overview of fundamentally SESAM modelocked optically pumped VECSELs. More details are listed in Tab. 1.

#140557 - $15.00 USD Received 4 Jan 2011; accepted 29 Mar 2011; published 13 Apr 2011

Table 1. Overview of fundamentally modelocked VECSELs.

number in Fig. 1	type	pulse duration	average output power	repetition rate	reference
1	MIXSEL	28.1 ps	6.4 W	2.5 GHz	[11]
2	MIXSEL	35.0 ps	40 mW	2.8 GHz	[5]
3	QW-VECSEL/QW-SESAM	4.7 ps	2.1 W	4.0 GHz	[10]
4	QW-VECSEL/QW-SESAM	6.1 ps	1.4 W	10.0 GHz	[20]
5	QW-VECSEL/QW-SESAM	3.3 ps	102 mW	50.0 GHz	[8]
6	QW-VECSEL/QD-SESAM	870 fs	45 mW	0.9 GHz	[15]
7	QW-VECSEL/QW-SESAM	260 fs	25 mW	1.0 GHz	[12]
8	QW-VECSEL/QW-SESAM	290 fs	10 mW	3.0 GHz	[21]
9	QW-VECSEL/QW-SESAM	477 fs	100 mW	1.2 GHz	[22]
10	QW-VECSEL/QW-SESAM	330 fs	120 mW	1.0 GHz	[23]
11	QW-VECSEL/QW-SESAM	190 fs	21 mW	3.0 GHz	[9]
12	QD-VECSEL/QW-SESAM	18 ps	27 mW	2.6 GHz	[19]
	this result 1 (QD/QD)	**416 fs**	**143 mW**	**4.5 GHz**	
	this result 2 (QD/QD)	**784 fs**	**1.05 W**	**5.4 GHz**	

2. VECSEL gain structure and SESAM

For all the results demonstrated throughout this paper, we used a specific SESAM-VECSEL combination where both elements were based on QDs. The semiconductor structure design of both elements and their relevant properties for modelocking, such as group delay dispersion (GDD) and non-linear reflectivity and temporal response of the saturable absorber, will be discussed in detail.

The QD-VECSEL gain structure (Fig. 2, left, Fig. 3, left) was grown at Innolume GmbH, Germany, by molecular beam epitaxy (MBE) on a gallium arsenide (GaAs) substrate. It consists of two distributed Bragg reflectors (DBRs) based on pairs of quarter wave layers of aluminum arsenide (AlAs) and aluminum gallium arsenide (AlGaAs). We use $Al_{0.2}Ga_{0.8}As$ instead of GaAs, although the refractive index contrast and therefore the reflectivity per DBR pair is lower in comparison, in order to circumvent unwanted pump absorption in these DBRs. The 15-pair DBR on the bottom of the structure was optimized to reflect the pump light at a wavelength of 808 nm (theoretical pump reflectivity > 99%), and the second 30-pair DBR to reflect the laser light at around 960 nm (theoretical reflectivity > 99.9%). We use an $Al_{0.2}Ga_{0.8}As$ spacer layer between the two DBRs of which we adjust the thickness and therefore shift the standing wave pattern of the electric field of the pump without influencing that of the laser. With this approach we can use this layer to optimize the structure for a maximum pump absorption in the active region where we achieve 90% of absorbed pump light. After the two DBRs, the active region is grown. It is mostly made up of GaAs, that serves as absorbing material for the pump radiation, in which 7 groups of 9 indium arsenide (InAs) QD layers are embedded.

The QD gain layers were grown using the Stranski-Krastanov growth method for self-assembled QDs. These groups of QD layers are distributed within the active region according to the standing wave pattern of the electric field of the laser. However, the positions of the individual groups are all optimized for slightly different laser wavelengths, resulting in a chirped positioning scheme of the active QD layers. The wavelengths we optimized the positions for are, in increments of 1.5 nm, 955.5 nm to 964.5 nm, with a design laser wavelength of 960 nm. In an additional step of optimization we calculated the spatially resolved pump absorption in the active region and superimposed it with the chirped positioning of the groups of QD layers. This results in a design of the active region where the specific group of QD layers optimized for the designed center laser wavelength of 960 nm is optimally placed at the position in the active region which exhibits the highest pump

#140557 - $15.00 USD Received 4 Jan 2011; accepted 29 Mar 2011; published 13 Apr 2011

absorption. Consecutively, the other QD layer groups are optimally positioned at anti-nodes of the corresponding chirped laser wavelength, placing a QD layer group with an optimization wavelength closer to the design wavelength in an area with higher pump absorption. After the active region we directly grew the semiconductor part of our anti-reflection (AR) section. It is a 14-layer AR section with twelve AlAs/$Al_{0.2}Ga_{0.8}As$ layers, a GaAs cap layer and a fused silica (FS) layer that was deposited using plasma enhanced chemical vapor deposition (PECVD).

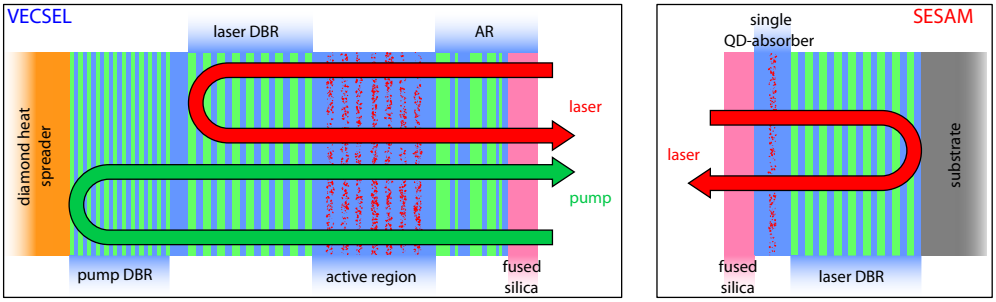

Fig. 2. Semiconductor designs of the QD-VECSEL (left) and the QD-SESAM (right).

The QD-SESAM (Fig. 2, right, Fig. 3, right) was MBE-grown on a GaAs substrate in the FIRST clean room facility at ETH Zurich. It was grown in normal order, starting with the DBR, and used with the 600-µm GaAs substrate. The anti-resonant QD-SESAM has a 30-pair DBR made of quarter wave pairs of AlAs and GaAs. The absorber section consists of a single InAs QD layer embedded in GaAs. The semiconductor part of the structure is finished resonantly but there is an additional quarter wave layer of PECVD-deposited FS on top, which results in an anti-resonant QD-SESAM design.

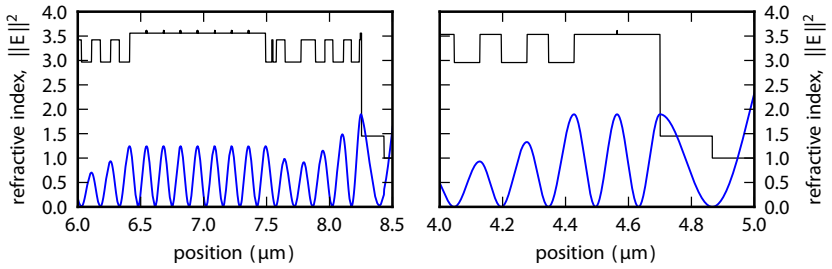

Fig. 3. Refractive index profile (black) and *E*-field distribution at a wavelength of 965 nm (blue) of the QD-VECSEL (left) and the QD-SESAM (right), showing the active and the absorber region, respectively, together with the top layers.

In order to emphasize the importance of this FS layer on top of the SESAM and also of the VECSEL's AR section (Fig. 2), we simulated the GDD of both devices with and without the corresponding top layers. The GDD as a function of the wavelength is shown in Fig. 4, on the left for the QD-VECSEL and on the right for the QD-SESAM. If we simulate the two structures without the AR section or the FS top layer, we obtain the black curves, reaching values of several 1000 fs^2. However, if we do the simulation with the top section we obtain a strong reduction of the GDD over a wavelength range of more than 30 nm (blue curves). In case of the VECSEL (left figure), the GDD with the AR section is also shown in red, however, it was multiplied by a factor of 1000 (corresponding to fs^2). This shows that the GDD of the VECSEL could be reduced to values between 0 fs^2 and 10 fs^2 over the entire wavelength range. To achieve such an improvement of the GDD, we implemented a Monte Carlo procedure combined with an additional least squares algorithm based on a transfer matrix method which optimizes the GDD of the structure. An important part of the design of

#140557 - $15.00 USD
Received 4 Jan 2011; accepted 29 Mar 2011; published 13 Apr 2011

our AR section is the last FS layer [24] without which the improvement in GDD would have been less pronounced.

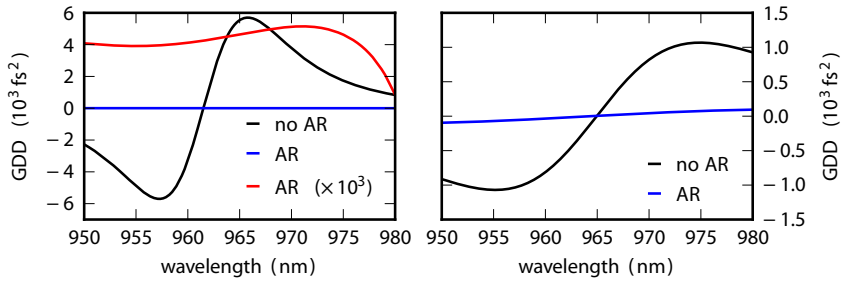

Fig. 4. GDD as a function of the wavelength for the QD-VECSEL (left) and the QD-SESAM (right). Left: Simulated GDD without top-coating (black), with top-coating (blue) and with top-coating and multiplied by a factor of 1000 (red). Right: Simulated GDD without top-coating and with top-coating (blue).

Low and flat GDD is required but not sufficient for shorter pulse duration [25]. In addition, optimized non-linear SESAM parameters are required. Therefore we determined the non-linear reflectivity and the temporal response of our QD-SESAM. In order to measure the non-linear reflectivity, we make use of a high sensitivity reflectivity setup [26]. The obtained data is then fitted with the function

$$R = R_{\mathrm{ns}} \cdot \frac{F_{\mathrm{sat}}}{F} \cdot \log\left(1 + \frac{R_{\mathrm{lin}}}{R_{\mathrm{ns}}} \cdot \left(\mathrm{e}^{F/F_{\mathrm{sat}}} - 1\right)\right) \cdot \mathrm{e}^{-F/F_2},$$

where R is the non-linear reflectivity, R_{ns} and R_{lin} the non-saturable and linear reflectivities, F_{sat} the saturation fluence and F_2 the induced absorption coefficient [27]. The result of the measurement is shown as blue dots in Fig. 5 on the left together with the corresponding fit in solid blue. From the fit we obtained the following parameters for the QD-SESAM: the saturation fluence was 3.8 μJ/cm^2, with non-saturable losses ΔR_{ns} (ΔR_{ns}=1 - R_{ns}) of less than 1% and a modulation depth ΔR (ΔR = R_{ns} - R_{lin}) of 1.2%. The induced absorption coefficient was also measured and it amounted to 24.7 mJ/cm^2. These values are highlighted in Fig. 5 as straight blue lines. The measurement was made at a laser wavelength of 965 nm with 180-fs pulses in a laser spot of about 18 μm in diameter. Since the probe pulses in this measurement are substantially shorter than the achieved pulse duration in modelocked configuration, the effect of induced absorption is significantly stronger in this measurement. At the achieved pulse duration in modelocked operation, the effect of induced absorption is not important since we operate the SESAM at fluences below 20 μJ/cm^2.

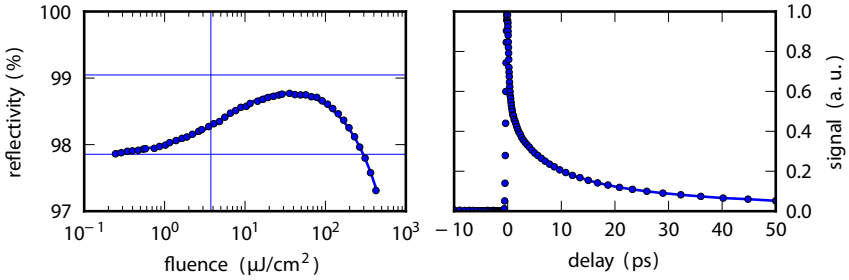

Fig. 5. Measurements of the non-linear reflectivity (left) and the impulse response (right) of the QD-SESAM. Left: Measurement points (blue dotted) and fit (solid blue). The solid thin blue lines are the fitted values for the parameters F_{sat}, R_{lin} and R_{ns}. (in the text). Right: Pump-probe measurement points (blue dotted) and double exponential fit (solid blue).

#140557 - $15.00 USD
Received 4 Jan 2011; accepted 29 Mar 2011; published 13 Apr 2011

The temporal response of the QD-SESAM was evaluated using a time resolved differential reflectivity setup where we used the same laser source as for the non-linear reflectivity measurement. As a function of the delay between the pump and the probe pulse the reflectivity of the sample changes and we obtain the curve shown in Fig. 5 on the right. The blue dots are the measurement and the solid blue curve the fit function. For fitting, we used a double exponential function of the form

$$A \cdot e^{-t/t_s} + (1-A) \cdot e^{-t/t_f},$$

in order to describe the relaxation behavior of QDs. The variables t_s and t_f, respectively, are the time constants of the slow and the fast exponential carrier decay, and A the ratio between their influence. From the fit we can determine those parameters and we find values of 15.9 ps and 500 fs for the slow and fast time constants, respectively. These values are comparable to previously realized QD-SESAM based on QD absorbers operating in the 1-µm spectral region, which achieved around 800 fs for the fast component [15].

3. Experimental laser setup and results

In order to obtain high power levels, it is crucial to optimize the thermal management [4]. Therefore, we used the thinned QD-VECSEL structure on a chemical vapor deposition (CVD) diamond of 450-µm thickness [28]. This so called "flip-chip bonding" is done by starting the structure growth from the GaAs wafer with an AlGaAs etch stop layer and then the actual QD-VECSEL structure is grown in reverse order. After that, the wafer is soldered to the CVD diamond and the substrate is removed by selectively etching the GaAs substrate using a citric acid hydrogen peroxide solution. In this way, an optimal thermal conductivity of the substrate of about 1800 $WK^{-1}m^{-1}$ can be reached, which is a significant improvement over other standard heat sink materials such as copper (Cu) (400 $WK^{-1}m^{-1}$).

For the experiments we used a simple v-shaped laser cavity (Fig. 6). The half opening angle of the laser with respect to the surface normal of the QD-VECSEL was about 10°. We used an output coupler (OC) with a transmission of 2.5% and a radius of curvature (ROC) of 100 mm. We applied the pump light perpendicularly to the QD-VECSEL in a pump spot radius of about 110 µm. In order to prevent over-saturation of the QD-SESAM we adjusted the cavity mode size on the SESAM with a SESAM-VECSEL distance of 3 mm. In this configuration we obtain close to identical mode sizes on both the SESAM and the VECSEL structure. We refer to this geometry as "one-to-one modelocking" [14] – well suited for further integration within a MIXSEL structure. According to our cavity simulations, the laser mode radii on the QD-VECSEL and on the QD-SESAM were 115 µm for the 5.4 GHz cavity and 119 µm for the 4.5 GHz cavity.

#140557 - $15.00 USD Received 4 Jan 2011; accepted 29 Mar 2011; published 13 Apr 2011

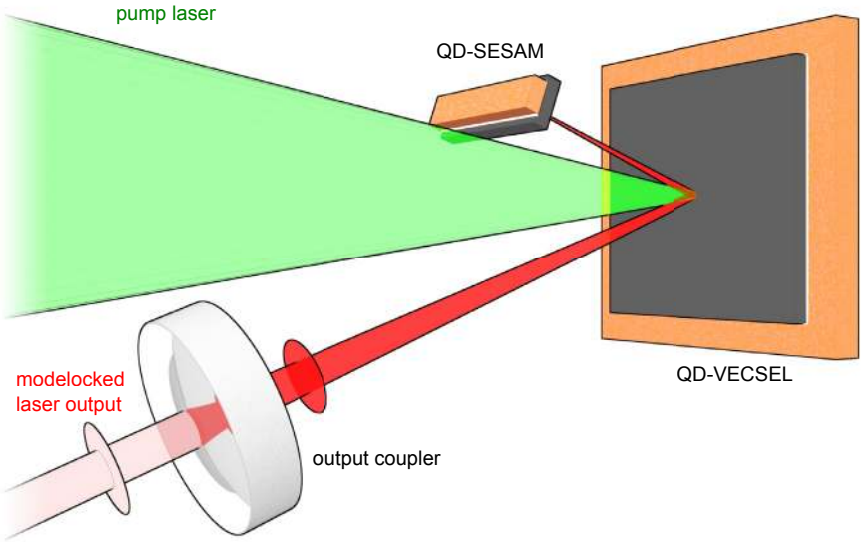

Fig. 6. Overview of the laser cavity, showing the perpendicular pumping geometry and the cavity elements: output coupler, QD-VECSEL and QD-SESAM.

The cavity configuration at 4.5 GHz corresponds to a cavity length of 33.6 mm. With a pump power of about 3.2 W we could generate 416-fs pulses (Fig. 7) at an average output power of 143 mW. The measured spectral width of the pulses was 2.7 nm, centered at around 960 nm (Fig. 7). This corresponds to a time bandwidth product (TBP) of 0.36, or 1.13 times the transform limit of a sech^2-pulse. During this experiment we had to cool the heat sink to about –24°C and the pulse fluence on the QD-SESAM amounted to 2.87 μJ/cm^2.

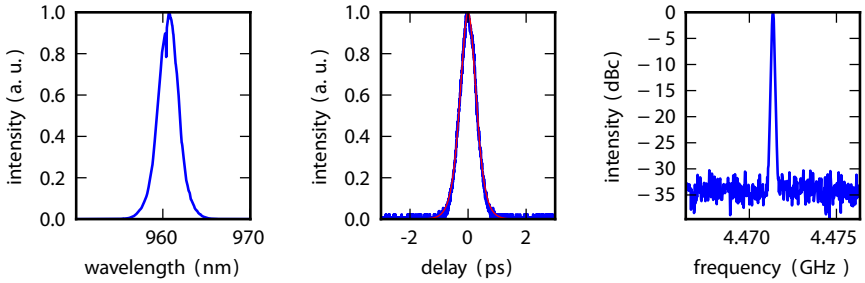

Fig. 7. Modelocking results for the shortest pulses obtained. Left: Optical spectrum with a spectral resolution of 0.2 nm and a spectral width of 2.7 nm around 961 nm. Middle: Measured auto-correlation trace (blue) and its sech^2-fit (red) showing a pulse duration of 416 fs. Right: Microwave spectrum with a resolution bandwidth of 100 kHz and a span of 10 MHz, showing a repetition rate of 4.47 GHz.

To increase the output power, we moved the OC closer to the QD-VECSEL to prevent over-saturation of the QD-SESAM. The cavity length was therefore adjusted to 27.6 mm, resulting in a repetition rate of 5.4 GHz. We pumped the QD-VECSEL with a power of about 11.7 W and we could observe 784-fs pulses with an average output power of 1.05 W (Fig. 8). During this experiment the heat sink temperature was about –20°C and the pulse fluence on the QD-SESAM was 18.4 μJ/cm^2.

#140557 - $15.00 USD
Received 4 Jan 2011; accepted 29 Mar 2011; published 13 Apr 2011

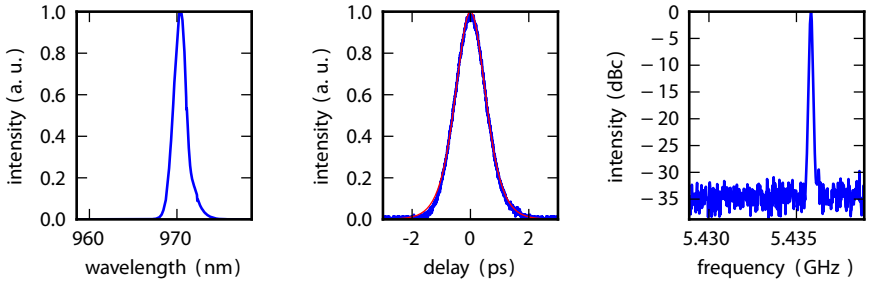

Fig. 8. Modelocking results of the highest average power obtained. Left: Optical spectrum with a spectral resolution of 0.2 nm and a spectral width of 1.7 nm around 970 nm. Middle: Measured auto-correlation trace (blue) and its sech^2-fit (red), showing a pulse duration of 784 fs. Right: Microwave spectrum with a resolution bandwidth of 100 kHz and a span of 10 MHz, showing a repetition rate of 5.44 GHz.

4. Conclusion and outlook

We have demonstrated a femtosecond QD-SESAM modelocked QD-VECSEL with 784-fs pulses at high average output power levels of more than 1 W. The VECSEL and the SESAM were both based on QD material for the active layers and the absorber layer, respectively. The key steps required for this achievement were the optimization of the QD-VECSEL and the QD-SESAM structures for low GDD, and in case of the QD-SESAM, also for fast recovery. This also enabled us to demonstrate the shortest pulses generated by a QD-VECSEL and also by a QD-SESAM. The shortest pulse duration was 416 fs at an average output power of 143 mW.

Currently the upper limit for high power scaling is an over-saturation of the SESAM and not a thermal rollover. We envision two different approaches to further improve the performance in the future. First, a larger laser mode area on both the QD-SESAM and the QD-VECSEL should result in an increased pulse energy and average output power. Second, a SESAM with a larger saturation fluence can be applied.

Our results clearly indicate how important it is to optimize the dispersion and SESAM recovery time in modelocked VECSELs. They are in good agreement with our experimental study on the influence of GDD on modelocked VECSELs [25]. However, further work is required to investigate the pulse formation process and the limitations in pulse durations and intra-cavity energy. In addition, at this point it is not clear that QDs are superior to QWs and further investigations should help to gain better insight here as well. Moreover, it will be very interesting to measure the gain bandwidth and temperature dependence for both structures.

This first demonstration of a Watt-level femtosecond VECSEL is a first milestone towards more compact high power femtosecond sources. We have operated both SESAM and gain structure with the same mode area, which will enable higher repetition rates and the MIXSEL integration. Therefore we expect that our gain and absorber structures can be fully integrated into a MIXSEL.

Acknowledgments

The research leading to these results has received partial funding from the European Community's Seventh Framework Programme (FAST-DOT) under Grant No. 224338, and by the Swiss Confederation Program Nano-Tera.ch which was scientifically evaluated by the SNSF.

#140557 - $15.00 USD Received 4 Jan 2011; accepted 29 Mar 2011; published 13 Apr 2011